

Energy transfer in multi-collision environments; an experimental test of theory: LiH (10;2) in H₂(0;0)

Article (Accepted Version)

Shen, Xiaoyan, Wang, Shuyin, Dai, Kang, Shen, Yifan and McCaffery, Anthony J (2017) Energy transfer in multi-collision environments; an experimental test of theory: LiH (10;2) in H₂(0;0). *Journal of Chemical Physics*, 146 (11). p. 114307. ISSN 0021-9606

This version is available from Sussex Research Online: <http://sro.sussex.ac.uk/id/eprint/71773/>

This document is made available in accordance with publisher policies and may differ from the published version or from the version of record. If you wish to cite this item you are advised to consult the publisher's version. Please see the URL above for details on accessing the published version.

Copyright and reuse:

Sussex Research Online is a digital repository of the research output of the University.

Copyright and all moral rights to the version of the paper presented here belong to the individual author(s) and/or other copyright owners. To the extent reasonable and practicable, the material made available in SRO has been checked for eligibility before being made available.

Copies of full text items generally can be reproduced, displayed or performed and given to third parties in any format or medium for personal research or study, educational, or not-for-profit purposes without prior permission or charge, provided that the authors, title and full bibliographic details are credited, a hyperlink and/or URL is given for the original metadata page and the content is not changed in any way.

Energy Transfer in multi-collision environments; an experimental test of theory: LiH (10;2) in H₂(0;0).

Xiaoyan Shen¹, Shuying Wang¹, Kang Dai¹, Yifan Shen²

¹School of Chemistry and Molecular Engineering, East China University of Science and Technology, Shanghai, 200237, China.

²School of Physics, Xinjiang University, Urumqi, 830046, China.

Email: shenxiaoyan73@ecust.edu.cn.

Anthony J. McCaffery,

Department of Chemistry, University of Sussex, Brighton, Sussex, BN16SJ, UK.

email. A.J.McCaffery@sussex.ac.uk.

Abstract.

We report separate experimental and theoretical studies that follow the equilibration of highly excited LiH ($v=10;J=2$) in H₂ at 680K. Experiments that follow the time evolution of state-to-state population transfer in multi-collision conditions were carried out by Shen and co-workers at Xinjiang University and East China Institute of Science and Technology with μ s resolution. At the same time, theoretical computations on the relaxation of this gas mixture were undertaken by McCaffery and co-workers at Sussex University. Rapid, near-resonant, vibration-vibration energy exchange is a marked feature of the initial relaxation process. However, at later stages of ensemble evolution, slower vibration-rotation transfer processes form the dominant relaxation mechanism. The physics of the decay process are complex and, as demonstrated experimentally here, a single exponential expression is unlikely to capture the form of this decay with any accuracy. When these separate studies were complete, the evolution of modal temperatures from the Sussex calculations were compared with experimental measurements of these same quantities from Shanghai and Urumqi. The two sets of data were found to be identical to within experimental and computational error. This constitutes an important experimental validation of the theoretical/computational model developed by the Sussex group and a significant experimental advance by the group of Shen et.al.

1. Introduction.

Research into the fundamental processes of collision-induced, energy transfer in the gas phase has a long history that is chronicled in a number of significant monographs ¹⁻⁵ and an extensive literature of research publications and reviews. Much experimental activity has involved the development of methods for creating single collision conditions through e.g. the use of molecular beam technology, to establish precise cross-sections and rate constants for the state-to-state transitions that constitute the elementary acts of collisional energy transfer. In a closely related strand of development, the application of lasers in collision dynamics experiments is now very widespread, extending the means by which accurate state-to-state rate constants and cross-sections may be measured for molecules in ground or excited states. In parallel to the evolution of experimental collision dynamics, there has been a similarly rapid and extensive development of theoretical methods of calculating state-to-state, single collision events, with a major early impetus provided by the formulation of a quantum scattering theory for atom – diatom collisions by Arthurs and Dalgarno ⁶ representing a theoretical benchmark. This emphasis on isolating the outcome of the single binary collision reflects the difficulty of experiment and of the standard theoretical methods that are widely used. Close Coupling calculations, classical trajectory methods and other variants are highly computer-intensive. As a result, real-life, multi-collision environments such as those found in planetary atmospheres, industrial plasmas etc. have, for the most part, been considered intractable at the most fundamental level. This is not wholly surprising. Gas phase energy transfer is a state-to-state process and typical gas ensemble may be one in which the collision rate exceeds 10^9 s^{-1} . Any attempt to model such an ensemble requires a fast, accurate collision theory and a method of tracking rotation and vibration population distributions throughout ensemble evolution. The experimental study of the multi-collision environment and the pathways of energy transfer in

large gas volumes also represent a daunting task that requires determination of quantum state population changes as a function of time on, at least, the μs scale.

The situation described above has recently changed in regard to both experimental and theoretical approaches to energy transfer. In 2002, Marsh and McCaffery⁷ reported the development of a computational model of state-to-state energy transfer in large, $\leq 10^4$ molecule, gas ensembles containing up to three different diatomic species. This development suggested that, for the first time, it might be possible to predict the quantum state-resolved pathways and outcomes of energy transfer in large gas mixtures computationally. This program has been used in a number of studies of energy flow in gas ensembles containing a small fraction of highly excited diatomic molecules in a variety of atomic and diatomic bath gases.⁸⁻¹² The evolution of these ensembles was followed to equilibrium in a series of collision cycles in which vibrational and rotational populations, as well as modal temperatures of vibration, (T_v) rotation (T_r) and translation (T_t), are available after each collision cycle or group of collision cycles. The result has enhanced insight into the principal energy relaxation mechanisms in the multi-collision regime. The computational/theoretical model used for calculating state-to-state collision-induced transition probabilities in gas ensembles is based on the angular momentum (AM) model^{13,14} of collision-induced, state-to-state energy transfer. In this method, in which the principal features were guided by experimental findings, the probability of converting linear-to-angular momentum (rotational and orbital) is calculated directly. This method results in a very simple form of mechanics in which the calculation of rotational transfer cross-sections is very fast and accurate.

In a separate, but related, development, the group of Shen et al. at XinJiang and Shanghai Universities have developed innovative experimental techniques that result in simultaneous spectroscopic and (μs) time-resolution of the changes in quantum state populations as highly excited gas mixtures equilibrate.¹⁵ Their experimental method was used to follow non-

equilibrium gas mixtures consisting of diatomic species, initially in very high states of excitation with collision partners (bath gases) in their ($v;j$) ground states.¹⁶ Their most recent experiments include that discussed here, in which LiH, initially in quantum state ($v=10; j=2$), represented in what follows as LiH (10;2), in a bath of H₂ (0;0). The details of these experiments are given in Section 2.

The experimental determination of state-to-state relaxation of LiH (10;2) in H₂ (0;0) with μ s time resolution, was undertaken in Xin Jiang and Shanghai. At the same time, theoretical computations were begun on the same gas mixture, and with constituents in the same initial quantum states, as those in the China-based experiments, were undertaken at University of Sussex. Only when these two investigations were complete were the experimental and computational results compared. In this publication we describe the results of experimental projects carried out by researchers at Shanghai and XinJiang Universities and those from the computational investigation at Sussex. It should be noted that the experiments carried out by Shen et al. are considerably more time-consuming and demanding than the, now, relatively straightforward and rapid computation of modal temperature evolution in the Sussex group.

1. Experimental methods

The apparatus used for the experiments is shown in Fig.1. A reaction cell containing Li metal is evacuated to 10^{-6} Torr prior to the introduction of 3 Torr of pure H₂, as measured by an MKS capacitance gauge. The cell was heated to 680K, at which temperature Li vapour pressure corresponds to 10 mTorr. A nitrogen laser-pumped dye laser operating at

$\lambda = 670.9\text{nm}$ was used to excite Li atoms to their 2p state. LiH $X^1\Sigma^+(v=0)$ is produced by the Li (2p)+H₂ reaction.¹⁵ A frequency-doubled YAG laser operating at 10Hz and pulse duration 5ns is used to pump an optic parametric oscillator (OPO). The OPO, which has the

frequency range 680-910nm and maximum pulse energy of 30mJ/pulse, excites LiH $X^1\Sigma^+(0,2)$ to $X^1\Sigma^+(10,2)$ by degenerate stimulated hyper Raman pumping (DSHRP)¹⁶. The OPO beam is delayed by about 2 μ s using a delay generator (DG535). In this brief delay time, LiH ($v=0$, J) rotational states are able to thermalize by collisions.

Using a tunable cw diode laser (DL100, 5mw, line width ~10 MHz) at $\lambda \sim 689$ nm, LiH $X^1\Sigma^+(10,2)$ was excited to its $A^1\Sigma^+(1,1)$ state and the resulting emission LiH $A^1\Sigma^+(1,1) \rightarrow X^1\Sigma^+(10,0)$ at 686.9nm, was transmitted through the monochromator located perpendicular to the laser beam. The monochromator (AM566, resolution 0.04nm) functions as a filter to reduce interference from scattered light. The detector signal was fed into an ICCD (DH734-18u-03, Andor) and the output recorded by the computer. The transition line profile for $X^1\Sigma^+(10,2) \rightarrow A^1\Sigma^+(1,1)$ was obtained by locking the diode laser to a fringe of the scanning interferometer and acquiring transient $A^1\Sigma^+(1,1) \rightarrow X^1\Sigma^+(10,0)$ intensities at approximately 40 discrete frequencies across the $X^1\Sigma^+(10,2) \rightarrow A^1\Sigma^+(1,1)$ transition line.

Rotational energy transfer in LiH (10,2)+H₂ collisions is investigated using the diode laser at $\lambda = 688-708$ nm. The $X^1\Sigma^+(10, J)$ state was excited to $A^1\Sigma^+(1, J+1)$. The laser induced fluorescence (LIF) intensity for transitions $A^1\Sigma^+(1, J+1) \rightarrow X^1\Sigma^+(0, J+2)$ was detected at right angles to the laser.

Collision-induced vibrational state change produces $X^1\Sigma^+(V < 10, 2)$ states. Using a cw Ti sapphire laser (Coherent MBR-110, 720-910nm, 450mw, linewidth < 5MHz), LiH transitions $^1\Sigma^+3, 'V(A \leftarrow X^1\Sigma^+(V \leq 10, 2))$ were excited by two-photon processes via the detection schemes shown in Table 1. From the LIF intensities and Franck-Condon factors, relative populations of Li ($V \leq 10, 2$) were $X^1\Sigma^+(V < 10, J \neq 2)$ transitions were not obtained. observed.

Table 1. Detection schemes of vibrational states of LiH

Vibrational state of $X^1\Sigma^+$	Detected transition	Franck-Condon factors[17]
0	X(0)-A(3) (372.26nm)	0.0326
1	X(1)-A(4) (386.6nm)	0.103
2	X(2)-A(3) (413.25nm)	0.0976
3	X(3)-A(2) (442.64nm)	0.0999
4	X(4)-A(9) (417.46nm)	0.0387
5	X(5)-A(9) (439.19nm)	0.0236
6	X(6)-A(14) (424.01nm)	0.0132
7	X(7)-A(14) (444.80nm)	0.0210
8	X(8)-A(17) (443.61nm)	0.0107
9	X(9)-A(19) (448.91nm)	0.0171
10	X(10)-A(22) (446.30nm)	0.0121

In the LiH+H₂ mixture, LiH $X^1\Sigma^+(10,2)$ were populated by the pulsed laser. The full state-resolved distribution of collisionally populated LiH molecules was determined by LIF on scanning the cw probe laser over the $X^1\Sigma^+(v) \rightarrow A^1\Sigma^+(v')$ transition, while the ICCD detected spectral line intensities and line shapes via the Fabry-Perot interferometer. The time between the end of the OPO pulse and the centre of the ICCD detection window, which is henceforth referred to as the “time delay” was varied. Using these techniques, clear and unambiguous pictures of the time evolution of the spectral line intensities and shapes were obtained.

3 Experimental results

3.1 Near-resonant V-V transfer

LiH (10,2) was excited by DSHRP. The diode laser intensity was reduced to 0.1 μW using filters (see Fig.1). The transmitted intensity $I_v(L)$ of the diode laser beam through vapour of length L is given by

$$\Delta I/I_v(0) = 1 - \exp[-k_{v',J' \leftarrow v,J}(\nu)L] \quad (1)$$

for light of frequency ν . Here $\Delta I = I_v(0) - I_v(L)$, $I_v(0)$ is the incident intensity and

$k_{v',J' \leftarrow v,J}(\nu)$ is the frequency-dependent absorption coefficient. Density [LiH (v,J)] is related to the integral of $k_{v',J' \leftarrow v,J}(\nu)$ by

$$\int k_{V',J' \leftarrow V,J}(v)dv = \frac{(\lambda_{V',J' \rightarrow V,J})^2}{8\pi} \frac{g_{J'}}{g_J} [LiH(V,J)] \Gamma_{V',J' \rightarrow V,J} \quad (2)$$

where $g_{J'}$ and g_J are the degeneracies of the J' and J state, respectively. $\Gamma_{V',J' \rightarrow V,J}$ is the natural radiation rate^{17,18} and $\lambda_{V',J' \rightarrow V,J}$ is the transition wavelength. The number density of excited LiH (10,2) molecules, $N_{v=10}$, was measured by scanning over the $X^1\Sigma^+(10,2) \rightarrow A^1\Sigma^+(1,3)$ transition at 688.77nm and monitoring transmission intensity. From the frequency-dependent absorption coefficient, the value $N_{v=10}=10^7\text{cm}^{-3}$ was obtained. Values of $N_{v<10}$ were acquired by replacing the diode laser with a titanium sapphire (TiSa) laser. This was used to excite LiH ($v \leq 10,2$) vibrational states by two-photon transitions with LIF detected by the ICCD. The measured LIF intensity I_v is proportional to N_v . Using the $X \rightarrow A$ data of Table 1, $N_{v<10}$ were obtained.

In a mixture of LiH ($v=10$) and H_2 ($v=0$) the following processes are near resonant:

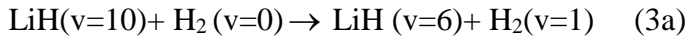
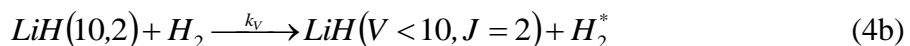
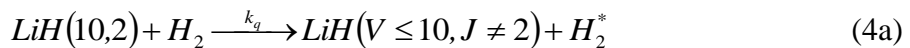


Figure 2 demonstrates that a significant fraction of the initial population of LiH ($v=10$) is rapidly transferred to the LiH ($v=6$) vibrational level. In this process, 4-1 resonant V-V energy transfer is observed in which four vibrational quanta are lost by LiH and one is gained by H_2 . Collisional energy transfer from LiH (10;2) to LiH ($v \leq 10, J \neq 2$), as depicted by Eq.(4a), represents all possible quenching pathways by H_2 and its rate is described using the rate constant k_q . Energy transferring in excitation of a specific vibrational and rotational state LiH ($v < 10, J=2$) occurs with the rate constant k_v , as shown in Eqn. (4b)



The time dependence of LiH ($v,2$) population can be written as ¹⁶

$$\frac{d}{dt} \left(\frac{[LiH(v,2)]_t}{[H_2][LiH(10,2)]_{t=0}} \right) = k_v e^{-k_q[H_2]t} \quad (5)$$

A plot of $\ln \left\{ \frac{d}{dt} \left(\frac{[LiH(v,2)]_t}{[H_2][LiH(10,2)]_{t=0}} \right) \right\}$ as a function of time delay produces a straight line of slope $= -k_q[H_2]$ and intercept $= \ln k_v$. An example of this analysis is shown in Fig.3.

A time window exists where Eq.(5) will be representative of our transient LiF signals. In order to establish this time window, we fit our data using Eq.(5) for times between 0 and 250ns. The k_v values for LiH (6;2) resulting from this analysis are shown in Fig.4. The figure indicates that values of k_v are constant only for approximately $t < 50$ ns. It is significant that the average time between collisions for the experimental condition used here is ~ 50 ns (single collision). The values decrease for times between 50 and 150ns, and become constant (but much reduced) for $t_D > 150$ ns. This result indicates that the rate constants do not have a constant value. Hence, a single rate constant is unlikely to capture the complex nature of V-V energy transfer processes.

In Fig.5, the results of this analysis are used to generate a model of transient LIF intensity for comparison with experimental data. The calculated data describe the experimental results very well out to $t = 50$ ns. This is expected because our kinetic model was developed by considering only those energy transfer events that occur immediately following excitation of LiH (10,2).

In order to demonstrate that the resonant energy exchange process (3a) really is essential for energy transfer between LiH ($v=10$) and H_2 , the time-profile of LiH ($v=6$) was measured following excitation of LiH ($v=10$). The result is shown in Fig.6 where two peaks are seen. The first peak is the result of multi-quantum (MQ) vibrational relaxation from $v=10$ to $v=6$

while the broader, lower, second peak is caused by transitions $v=10 \rightarrow v=9 \rightarrow v=8$ $v=7 \rightarrow 6$ transfer, referred to as sequential, single quantum relaxation (SSQ).

Fig.7 demonstrates that significant fractions of the initial population of LiH (10,2) are transferred to LiH (6,2), LiH (2,2) and LiH (0,2) rovibrational levels after delays $t_D=0.25 \mu s$ and $0.5 \mu s$. Since the average time between collisions is $\sim 50 ns$, data following 5 collisions ($t_D=0.25 \mu s$) and 10 collisions ($t_D=0.5 \mu s$) are obtained. The time-scale of these transfer processes is far shorter than sequential single-quantum collisional lifetimes (see Fig.6). Near-resonant V-V energy transfer is clearly observed.

After $t_D=0.5 \mu s$ rovibrational populations of LiH ($v \leq 10, v=2$) represent Boltzmann distributions. In Fig.8, the vibrational temperatures of 6400 ± 10 , 4600 ± 10 and $3000 \pm 240 K$ are those for time delays $5 \mu s$, $10 \mu s$ and $30 \mu s$, respectively. The full experimental decay curve of T_{vib} for LiH (10;2) in a bath of $H_2(0)$ at 680K is displayed in Fig.9.

Note that N_v (LiH) is the density of LiH ($v \leq 10, J=2$) molecules, and G_v is the vibrational

$$\text{energy given by }^{17} G(v) \text{ (LiH)} = 1405.91 \left(v + \frac{1}{2} \right) - 23.18 \left(v + \frac{1}{2} \right)^2 + 0.18 \left(v + \frac{1}{2} \right)^3$$

3.2 Rotational (T_r) and translational (T_t) temperatures of LiH (10,2) in H_2 .

Laser-induced fluorescence (LIF) intensities for individual rotational states of LiH (10, J) were measured following excitation of LiH (10;2). These intensities were integrated over the Doppler-broadened, transient LIF line widths. The LIF signals were converted to rotational populations using the appropriate Honl-London factors. Rotational populations were found to approximate to Boltzmann distributions. The slopes of plots for each transient rotational population versus $J(J+1)$ yields the corresponding T_r as shown in Fig.10.

LIF line profiles of the LiH (10,2) rotational state were used to determine the distributions of translational temperatures (T_t). The transient line profiles are well described by single Gaussian distributions. The laboratory frame translational temperatures are calculated using the relation

$$T_{trans}(K) = \left(\frac{mc^2}{8k \ln 2} \right) \left(\frac{\Delta \nu}{\nu_0} \right)^2 \quad (6)$$

Here m is the mass of LiH, k is the Boltzmann constant, c is the speed of light. $\Delta \nu$ is the full width half maximum of the transition profile and ν_0 is the transition frequency. The temperatures T_t for LiH (10,2) state are all greater than 680K.

The time evolution of T_r and of T_t for LiH (10;2) in H_2 are shown in Fig.12. T_r was found to peak within the first few μs and thereafter, slowly decreases, finally equilibrating to a temperature slightly lower than that of the cell, ($T_{cell} = 680K$).

That change in rotational state population accompanies vibrational state change is not surprising. The initial V-V exchange will generally not be precisely energy-resonant with the vibration state change in H_2 and so rotational state change would be needed to ensure energy conservation in combined LiH de-excitation- H_2 excitation. For example, for the process $LiH(10,2) + H_2(0,0) \rightarrow LiH(2,2) + H(2,0)$, ΔE , the energy defect, $= 755 cm^{-1}$. This energy will be transferred to rotational states of LiH ($10, J > 2$). Hence the peak in T_r . Fast, multi-quantum vibrational relaxation of highly vibrationally excited LiH ends after time delay of $10 \mu s$. T_r then slowly decreases. We see that T_t increases monotonically as a function of t_D . This behaviour is consistent with the angular momentum model for collisional energy transfer (see section 4).

3.3. T_v of the H_2 bath gas

Due to the processes described in detail in sections **3a** and **3b**, we may assume the populations of $H_2(v=1)$, $H_2(v=2)$, and $H_2(v=3)$ approximately equal those of LiH ($v=6$), LiH

($v=2$), and LiH ($v=0$) respectively. On plotting $\ln N_v(\text{H}_2)$ as a function of vibrational energy $G_v[\text{H}_2(v)]$ for collisions of LiH($v=10$) with $\text{H}_2(v=0)$, the slopes yield the Boltzmann vibrational temperatures shown in Fig.13.

Fig.14 shows the evolution of modal temperatures of LiH (10,2) in a bath of H_2 initially at 680K, as well as that of T_v for H_2 . Each modal temperatures is plotted as a function of pump-probe delay time. T_v for LiH falls very rapidly while that of H_2 rises sharply for the duration of the near resonant V-V energy transfer. Following this initially rapid energy exchange there is slow equilibration as SSQ processes begin to dominate.

4. The computational model.

The computational model used by the Sussex group to follow state-to-state energy transfer in the LiH (10;2) in H_2 (0;0) 1:1 ratio mixture through series of collision cycles, was briefly referred to in the Introduction section. A number of recent publications⁸⁻¹² have described the basis of the model and how it is used, and only a brief description is given here. The system of mechanics used for determining the outcome of individual diatomic-diatomic, or atom-diatomic collisions is the angular momentum (AM) model of collision - induced state change. This fast, accurate, theoretical method was developed by McCaffery and co-workers^{13,14} following a series of experiments designed to reveal the motive force for quantum state change in molecular collisions. These experiments, and the conclusions drawn from them, have been described in a recent review.¹⁹ It was concluded that the principal driving force in diatomic – diatomic, and atom – diatomic energy transfer collisions is *momentum change*, particularly linear-to-angular (orbital and rotational) momentum conversion. In the AM model, the probability of angular momentum change is calculated directly within constraints set by state-to-state and overall energy conservation. The result is a fast, accurate method of calculating rate constants and/or cross-sections for state-resolved energy transfer.

The AM method forms the basis of a multi-collision, computational model of energy transfer in large $\leq 10^4$ molecule, gas ensembles containing up to three different species that was developed by Marsh and McCaffery.⁷ In this computer program, molecules of a chosen species are set initially to be in specific, excited rovibrational states at a specified collision energy or Boltzmann distribution at specific temperature. Pairs of molecules are selected for collision at random following which, the post-collision quantum state populations are recorded. This process is carried out 10^4 times to constitute a single collision cycle. Collision cycles may be repeated singly or in groups. After each, the ensemble component data that are available for download include vibration and rotation state populations for each species present and the modal temperatures of each. When plotted against number of collision cycles, the modal temperatures are useful in visualising the equilibration process as they compress a large amount of data into a single set of quantities, the T_m for each constituent.

In the case of the ensemble considered here, LiH (10;2) is present as a 1:10 ratio component in a bath gas of H₂ (0;0) at collision energy 680K. Calculations were carried out in the manner described above and the evolution of modal temperatures of LiH and that for T_v of H₂, the bath gas, are shown in Fig.12. As discussed above, these data are initially computed in terms of modal temperature as a function of number of collision cycles. The results are straightforwardly converted to a μ s scale for comparison with the experiment using the gas cell pressure reported by Shen et al.

Discussion and Conclusions.

This work describes two different approaches, one theoretical and the other experimental, each designed to follow state-to-state energy transfer in multi-collision gas phase environments. Studies carried out thus far suggest that much can be learned about energy flow in gas ensembles from such research. The experiments described above, and earlier

studies by Shen et al.¹⁵ have demonstrated it is possible to follow the equilibration of gas mixtures containing highly excited molecules with state-to-state resolution. This experimental advance, and the closely related theoretical modelling of relaxation of excited molecules in the multi-collision environment by McCaffery et al.,⁸⁻¹¹ are of wide significance as they demonstrate that the fundamental state-to-state processes of energy transfer between molecules in highly excited states may be identified and predicted, even when these molecules are minority components in large gas volumes. This takes the field of experimental and theoretical collision dynamics beyond the single collision regime, indicating that it is feasible to have detailed understanding of energy transfer in gas ensembles of technological, industrial, environmental and interstellar interest. The experimental study of equilibration of LiH (10;2) in H₂ (0;0) described above, represents a detailed and thorough, multi-experimental investigation in which key elements are rigorously examined.

In the work described in this publication, theoretical computations by McCaffery in Sussex University and experimental pump-probe methods by Shen et al. in XinJiang and Shanghai Universities were separately employed in studying energy transfer in identical gas mixtures, namely that of LiH (10,2) in H₂ (0;0) at collision energy = 680K. The data from these separate investigations, plotted as the modal temperatures of T_v, T_r and T_t for LiH and that of T_v for the H₂ bath gas, are shown in Figs 11 and 12. It is immediately evident that the two sets of data are very similar indeed with close agreement on peak values as well as equalisation points. This represents a substantial achievement by the computational model as, by the time the final stages of ensemble evolution in Fig. 12 have been reached, more than 10⁷ binary collisions will have taken place within the ensemble.

The study of the equilibration of LiH (10;2) in H₂ (0;0) by Shen et al. demonstrates that state-to-state energy transfer may be followed experimentally in multi-collision environments.

This constitutes a significant advance towards a detailed understanding of energy flow in large gas mixtures. There is close agreement between the data of Shen et al. and results obtained by McCaffery using the theoretical/computational model devised by Marsh and McCaffery.⁷ This represents a validation of the computational model. In light of the number of binary collisions undergone in a typical computational run, this close agreement implies that the underlying collision physics, i.e. the AM model,^{13,14} represents the outcomes of individual diatom-diatom collisions with considerable accuracy.

This and earlier studies⁸⁻¹² allow some conclusions to be drawn regarding the dominant processes of gas phase energy transfer when many collisions occur. A striking feature is the near-resonant V-V exchange process, found when a transition downwards in energy within the excited molecule's vibrational manifold is in near-energy coincidence with one upwards in energy from the ground state of the bath molecule. This is generally a multi-quantum (MQ) exchange process during which rapid vibrational deactivation occurs, generally for a short period. This is not an original observation though this and related studies²⁰ indicate the presence of an unexpected ubiquity and predictability for this rapid energy exchange process. However, it is evident that near-resonant V-V does not appear to be the major deactivation process as Fig.6 demonstrates. Despite the efficiency of the rapid, initial V-V exchange, the principal relaxation mechanism appears to be the slower, single sequential quantum (SSQ) vibration-rotation exchange process. This is a relatively inefficient process because of the exponential-like fall of rotational transfer probabilities as the magnitude of rotational state change increases.

Acknowledgement

The experimental component of this study was partially supported by the National Natural Science Foundation of China (No. 11164028 and 11364042).

References.

1. J. D. Lambert, *Vibrational and Rotational Relaxation in gases*, Clarendon Press, Oxford (1977).
2. R. D. Levine and J. Jortner, *Molecular energy transfer*. Wiley, New York (1976)
3. J. T. Yardley, *Introduction to Molecular Energy Transfer*, Academic Press, New York, (1980).
4. R. D. Levine and R. B. Bernstein, *Molecular Reaction Dynamics and Chemical Reactivity*. Oxford University Press, Oxford (1987).
5. R. D. Levine, *Molecular Reaction Dynamics*. Cambridge University Press, Cambridge, (2005).
6. A. M. Arthurs and A. Dalgarno, Proc. Roy. Soc. **A256** 540 (1960).
7. R. J. Marsh and A. J. McCaffery, J. Chem. Phys., **117**, 503 (2002).
8. A. J. McCaffery, J. Chem. Phys., **144**, 044317, (2016).
9. A. J. McCaffery, M. Pritchard, J. F. C. Turner and R. J. Marsh, J. Chem. Phys., **134**, 194304 (2011).
10. A. J. McCaffery, J. Chem. Phys., **143**, 104306 (2015).
11. A. J. McCaffery and R. J. Marsh, J. Chem. Phys., **139**, 234310 (2013).
12. M. Pritchard and A. J. McCaffery, J. Phys. Chem A, **116**, 2006, (2012).
13. M. A. Osborne and A. J. McCaffery, J. Chem. Phys., **101**, 5604 (1994)
14. A. J. McCaffery, Z. T. AlWahabi, M. A. Osborne and C. J. Williams, J. Chem. Phys., **98**, 4586 (1993).
15. Jye-Jong Chen, Yu-Ming Hung, Dean-Kuo Liu, Hok-Sum Fung and King-Chuen Lin, J. Chem. Phys. **114**, 9395 (2001).
16. A. Alghazi, J. Liu, K. Dai, and Y. F. Shen, Chem. Phys. **448**, 76 (2015)

17. W. T. Zemke and W. C. Stwalley, J. Chem. Phys. **68**, 4619(1978);
18. W. C. Stwalley, W. T. Zemke, J Phys. Chem. Ref. Data **22**,87(1993.)
19. A. J. McCaffery, Phys. Chem., Chem. Phys. **6**, 1637, (2004).
20. C. Ottinger, A. F. Vilesov, and D. D. Xu, J. Chem. Phys, **102**, 1673, (1995).
21. R. Bachmann, X. Li, C. Ottinger and A. F. Vilesov, J. Chem. Phys., **98**, 8606, (1993).
22. J. A. Mack, K. Mikulecky and A. M. Wodtke, J. Chem. Phys., **105**, 4105, (1996).
23. C. S. Parmenter, S. J. Clegg, D. Krajnovich and D. Lu, Proc. Nat. Acad. Sci., **94**, 8387 (1997).
24. L. G. Piper, J. Chem. Phys., **101**, 10229, (1994).
25. G. Flynn, Acc. Chem. Res. **14**, 334 (1981).

Figure Captions

Fig. 1 OPO: optical parametric oscillator; M: monochromator; DM: dichroic mirror; BS: beam splitter; FPI: Fabry-Perot interferometer; P.D: Photodiode; R.F: removable filter; R.M: removable mirror; F.O: Fiber optic.

Fig.2. Direct evidence for 4-1 resonance in LiH ($v=10$)+H₂ ($v=0$). Initial preparation of LiH ($v=10$) results in slow population of LiH ($v=9$) but rapid, direct population of LiH ($v=6$).

Fig. 3 Linear least squares fit of early-time, transient data using Eq.(5) for the appearance of LiH (6,2). Here, $y = [LiH(6,2)] / [H_2][LiH(10,2)]_{t=0}$, slope= $-k_q[H_2]$.

Fig.4 State-resolved energy transfer rate, k_v , with error bars, for energy gain into the LiH (6; 2) as a function of time, included in the fit to Eq.(5). Values for k_v were determined by fitting the transient LIF data for LiH (6,2) to Eq.(5) and including various time intervals in the fit

Fig.5. Comparison of the transient LIF intensity signal for LiH (6;2) following collisions with LiH (10;2) with results from fitting the data to a kinetic model [see Eq.(5)].

Fig.6 Time-profile of population growth in $v=6$ following excitation of $v=10$ of LiH. The first peak is due to multi-quantum (MQ) relaxation. The second, broader, peak is due sequential single quantum (SSQ) relaxation.

Fig.7. Rovibrational state populations of LiH ($v,2$) after 5 and 10 collisions. Note that at these stages, the populations of unexcited $v=0$ are very small. The effect of near resonant V-V transfer is clearly evident in $v=6$ and $v=2$ populations. The modal temperatures T_v were obtained by dividing the mean vibration energies the appropriate multiples of k . (a) mean vibration energy $E_{vib} \sim 12200 \text{ cm}^{-1}$ yields $T_{vib} = 17600 \text{ K}$ (b) $E_{vib} \sim 11090 \text{ cm}^{-1}$ yields $T_{vib} = 16000 \text{ K}$

Fig.8. Plots of $\ln[N_v(\text{LiH})]$ as a function of $G(v)(\text{LiH})$. The slopes are a measure of $T_v(\text{LiH})$.

Fig.9. Experimental vibrational temperature (T_{vib}) as a function of time for LiH (10,2) in H_2 at 680K.

Fig.11 Doppler-broadened transient line shapes for LiH (10,2).

Fig.10. Rotational distributions (T_r) for LiH ($v=10, J=0-13$) states resulting from collisions with H_2 . For each plot, slope = $-B/kT_{rot}$, and for $B_{v=10}$, the rotational constant for LiH = 5.241 cm^{-1} .

Fig.11 shows the transient profiles at delays 10 and 20 μs following the OPO pulse.

Fig. 12. Evolution of modal temperatures of vibration T_v (black squares) rotation T_r (red circles) and translation T_t (green triangles) for LiH and T_v for H_2 bath gas (red triangles).

Note that the data were initially computed in terms of collision cycles and converted to

graphs of T_m versus pump-probe delay time using the experimental gas pressures reported by Shen et al.

Fig.13 Plot of $\ln [N_v(H_2)]$ as a function of $G_v(H_2)$. The slopes constitute a measure of T_v for H_2

Fig.14 Evolution of modal temperatures of $LiH(10,2)$ and of T_v for H_2 , in a bath of H_2 at 680K plotted as a function of pump-probe time delay.

.